

## **APPENDIX B**

**“A fast Scanner for Fluorescence Microscopy Using a 2-D CCD and Time Delayed Integration” by Netten, *et al.*, Bioimaging 2 (1994) 184-192 (“Netten”)**

# A fast scanner for fluorescence microscopy using a 2-D CCD and time delayed integration

Hans Netten†, Lucas J van Vliet, Frank R Boddéke, Peter de Jong and Ian T Young

Pattern Recognition Group of the Faculty of Applied Physics, Delft University of Technology, Lorentzweg 1, 2628 CJ Delft, The Netherlands

Submitted 22 August 1994, accepted 12 October 1994

**Abstract.** We have developed an imaging system for high speed image acquisition in fluorescence microscopy. The use of a two-dimensional CCD array in a special operation mode called TDI (Time Delayed Integration) permits a significant increase in photon integration time compared to 1D scanners (higher signal-to-noise ratio) without compromising the total data throughput rate. Instead of a start-stop system we use continuous stage motion in the CCDs parallel shift direction. Synchronizing the parallel clock and the stage velocity guarantees a one-to-one relationship between a moving cell and its image onto the CCD. Compared to start-stop systems, TDI scanning offers a speed improvement, negligible blurring in the scanning direction and a complete suppression of pixel variability boosting the SNR more than 10 dB.

**Keywords:** TDI, signal-to-noise ratio, fluorescence microscopy, CCD camera, spatial frequency response.

## 1. Introduction

Image cytometry—while it offers the opportunity for accurate and precise measurement of cell properties as well as confirmation of detection—has been limited to small sample sizes. In a number of important areas the need for instrumentation for high-speed measurement of cells and cellular constituents has outstripped available systems. In modern molecular cytogenetics, techniques have been developed to selectively label various DNA sequences with fluorescence tags in interphase as well as metaphase cells. This technique is called fluorescence *in situ* hybridization (FISH) (Carter 1994). FISH makes it possible to detect structural chromosomal abnormalities in metaphase spreads. Structural abnormalities include translocations, amplifications and deletions. FISH also allows large scale screening to detect an abnormal copy number of a specific chromosome in interphase cells. In order to obtain a reliable estimate for the frequency of occurrence a large number of cells needs to be analysed (Netten *et al* 1994).

A bottleneck in fluorescence image cytometry is the low intensity of fluorescently labeled probes. Often intensified CCD cameras are used to deal with low light levels. But such systems do not have the proper characteristics, because the intensifier causes a boost of the photon shot noise and reduces the spatial resolution. Low intensities require special cameras that are capable of accumulating signals, for tens of seconds. A slow-scan cooled CCD camera has the required characteristics. Such a camera offers a linear photometric response over a large intensity range, cooling that effectively suppresses the dark current to allow long integration times and a slow readout rate to provide a low readout noise.

Traditionally, automated systems capture images field after field. Image acquisition (exposure and readout) and stage movement from one field to the next field takes place during the processing time of the previous image. The stage movement starts directly after the exposure, during readout. Using a slow-scan CCD camera the stage motion will be finished before the readout is completed. Real-time image processing can be achieved when the processing time is

† To whom correspondence should be addressed.  
e-mail: hannesgh@utw.delft.nl

‡ Real-time means a rate such that the previous image is processed before the next image is offered. Sometimes this means video rate.

shorter than the total time needed for image acquisition and stage movement. Throughout this paper this field approach will be referred to as static image cytometry. In *dynamic* image cytometry there is a continuous flow of data that is processed and analysed in real-time. As a consequence, the microscope stage moves non-stop to offer new scenes at the input of the system. Dynamic imaging systems have been developed for bright field microscopy (Stark *et al* 1989, Tüchter *et al* 1987). These imagers make use of a one-dimensional linear CCD and are not suitable for low light intensities. The data throughput will be very low for long integration times. Using a two-dimensional CCD combined with time-delayed-integration a high data throughput is possible without compromising the integration time.

A number of time-delayed-integration imagers have been reported in the literature (Schlig 1986). These scanners are designed to be used for page and document imaging. Special TDI CCD sensors are used to achieve high speed and signal-to-noise ratio even with low light levels (Barbe 1976). The TDI sensors are characterized by the width of the array (serial dimension) and the number of stages (parallel dimension). Typical example of such an array is  $2048 \times 96$  TDI chip. Signal level increases as the number of TDI stage increases whereas the total noise level increases by the square root of the number of stages (Chambarlain and Washkurak 1990).

We have designed a TDI scanner suitable for fluorescent image cytometry. It is built around a slow-scan cooled CCD camera that is normally used for static imaging. This paper presents the design and performance of such a system. The paper is organized as follows. In section 2 we describe the principle of TDI scanning. Section 3 gives a summary of the design parameters. The actual implementation is presented in section 4. We have evaluated the scanner by measuring the SNR, spatial frequency response and speed. The experimental results are given in section 5. Finally, in section 6 we draw some conclusions.

## 2. TDI scanning principle

A CCD element consists of a two-dimensional matrix of square photosensitive sites, the electron wells. This matrix is called the parallel register. The CCD contains a second register, the serial register, which is itself a one-dimensional CCD and plays an important role during CCD readout. In the operation of a full frame CCD we distinguish two stages: the integration time in which the exposure takes place, and the readout time. When sufficient photon-induced electrons have been collected in the various CCD wells, the CCD is ready for readout. During the readout time all charge stored in the parallel register is shifted (in parallel) towards the serial register. Each cycle the parallel clock causes a shift of exactly one row. The charge stored in the top pixel row is shifted from the parallel register into the serial register. Once in the serial register, the serial

or pixel clock transfers the charge packets to the amplifier and A/D converter. After the serial register is emptied the whole cycle of a parallel shift followed by serial readout is repeated until the parallel register is emptied (Aitkens *et al* 1990).

TDI scanning combines the light integration with the CCD readout into a continuous process. During integration the continuous movement of the stage is synchronized with the parallel shift of the CCD. At each parallel clock cycle a new row of pixels at the bottom of the CCD is exposed by a new scene. As the scene moves, the corresponding row also shifts in the same direction at each cycle of the parallel clock. Finally this row reaches the top of the CCD and is shifted into the serial register and then to the A/D converter. Figure 1 shows three steps of TDI scanning. Considering the black pixel in the left-most column, the pixel shifts towards the serial register synchronized with the motorized stage. The pixel integrates from the bottom of the CCD until it reaches the serial register. TDI scanning permits continuous movement of the stage (high throughput) without compromising the photon integration time (high SNR). This leads to a continuous pixel stream during the integration. The result is an image of  $S \times N$  pixels, where  $S$  is the serial dimension of the CCD and  $N$  can be extremely long.

## 3. TDI Scanning parameters

To avoid unnecessary blurring, both the scanning speed and the scanning direction need to be controlled. TDI scanning requires precise alignment between the parallel shift direction of the CCD and the direction of stage movement. The integration time can be controlled by adjusting the stage velocity and shift frequency. The values for the parallel clock and the stage velocity depend on the camera and the microscope setup. For a required total integration time  $T_i$  (that is dependent upon specimen brightness), the parallel shift frequency  $f_p$  is given by:

$$f_p = \frac{P}{T_i} \quad (\text{Hz}) \quad (1)$$

where  $P$  is the parallel dimension of the CCD chip. With a frequency  $f_p$  a row of pixels shifts from the bottom to the top of the CCD in  $T_i$  seconds. As the CCD shifts one pixel the stage must move one pixel distance divided by the magnification. The stage velocity is given by:

$$v_s = \frac{P \Delta}{T_i M} = \frac{f_p}{f_o} \quad (\mu\text{m s}^{-1}) \quad (2)$$

where  $M$  is the total magnification,  $\Delta$  is the pixel size and  $f_o$  is the spatial sampling frequency of the microscope system. The spatial sampling frequency can be measured with a bar pattern on a test slide. Using a zoom projection lens, each time the magnification changes the sampling frequency must be measured, therefore a fixed

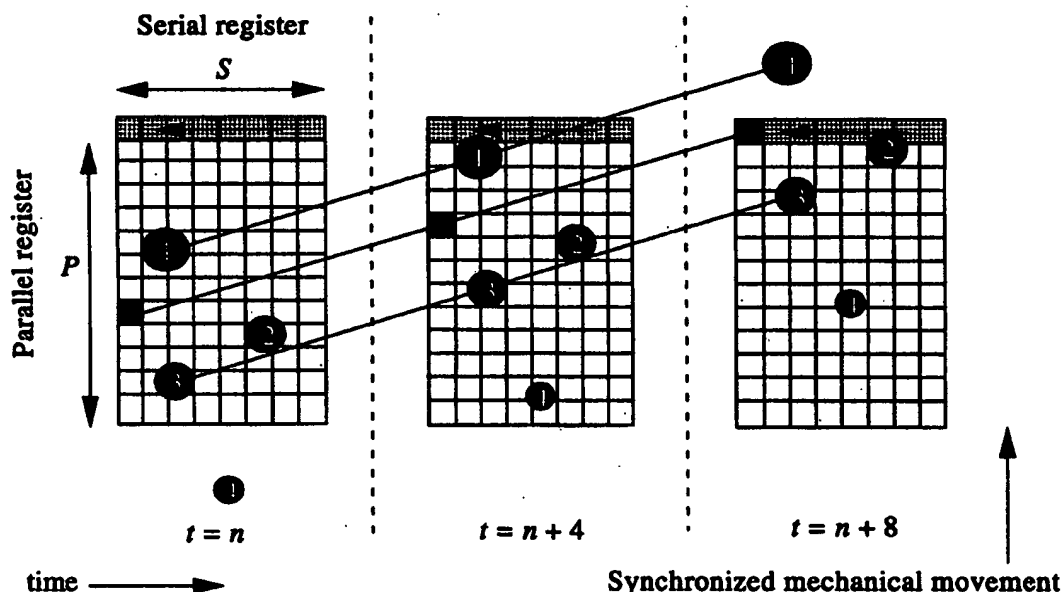


Figure 1. Three stages of TDI scanning at intervals separated by 4 cycles of the parallel clock. The numbered black dots are moving upwards and are imaged on a CCD matrix.

magnification is to be preferred. In our system there is no position feedback from the stage to control the camera shift. Therefore the stage velocity as well as the shift frequency must be very stable and accurate.

The maximum readout rate ( $r_{\max}$ ) of the camera limits the shift frequency and stage velocity. Given equation (1), the upper bound of the shift frequency is given by:

$$f_p < \frac{r_{\max}}{S} \quad (\text{Hz}) \quad (3)$$

where  $S$  is the serial dimension of the CCD. Due to the upper bound of the shift frequency the integration time is limited by a lower bound and is given by:

$$T_i > T_r = \frac{S}{r_{\max}} \quad (\text{s}) \quad (4)$$

$T_r$  is the readout-time of the camera to acquire a full image. A shorter integration time than the readout time is not possible with TDI scanning. If a shorter integration time is required due to saturation of CCD wells, the emitted light must be reduced. An optical neutral density filter is a common way to reduce the photon flux but, in practice, strong FISH signals are extremely rare.

The scanning speed is defined as the total area that is scanned per second. Each second  $S$  times  $f_p$  pixels are acquired. The number of pixels divided by the spatial sampling density squared gives the area that is scanned per second. Combining this result and equation (1) yields the

scanning speed:

$$v_{\text{TDI}} = \frac{PS}{T_i f_c^2} \quad (\mu\text{m}^2 \text{ s}^{-1}) \quad (5)$$

Equation (5) shows that the scanning speed is determined by the required integration time, sampling density and the dimension of the selected CCD. Because of the limitation of the readout rate the maximum scanning speed is achieved when the integration time is equal to the readout time of the camera. Typical values for all of these variables will be presented in the following section.

## 4. System Implementation

### 4.1. Hardware

Our TDI scanning system is built around a Nikon Diaphot epi-illuminated inverted microscope. The microscope is fully automated. Focus, stage, camera and excitation shutter are controlled by a computer. Figure 2 shows a schematic diagram of the system.

The microscope is equipped with a motorized stage. The stage is driven by two DC motors. Each motor has a position encoder that is part of a closed loop system, controlled by a digital Proportional Integral Derivative filter (PID, model LM 628, National Semiconductors) (Warwick and Rees 1988). One encoder step size is 50 nm. TDI scanning requires a constant velocity of the stage. Our experiments have shown that stepping motors are not

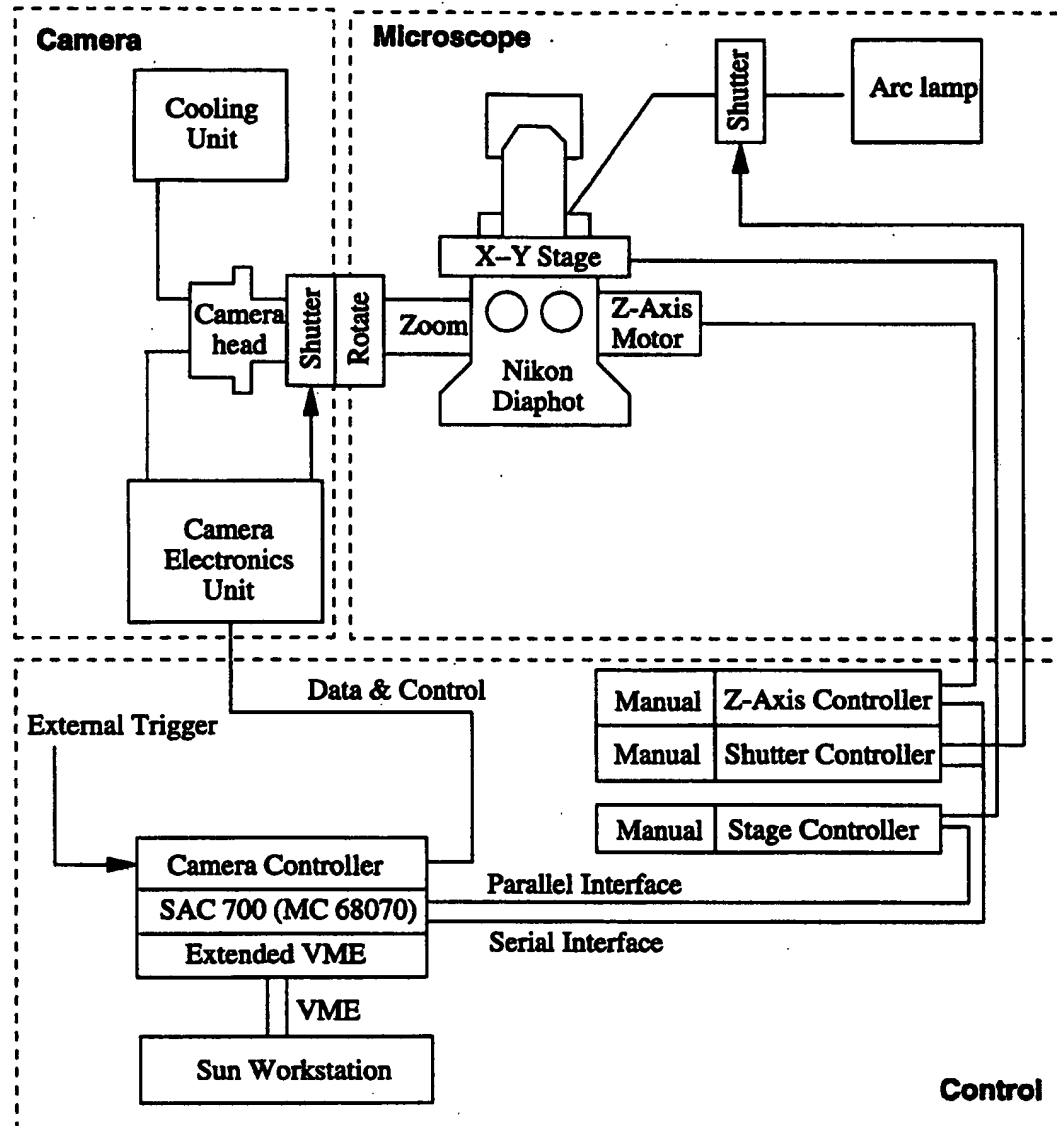


Figure 2. Schematic overview of a TDI scanning system. The dashed lines separate the camera, microscope and control unit.

suitable for this application. With DC motors the stage velocity is more stable. The PID filter cannot compensate for mechanical disturbance of the stage because the stage is not included in the close loop. The encoder gives the position of the motor and not of the stage. Therefore precise mechanics is used to connect the motors and the stage. Focus control is also driven by a DC motor with a PID filter. Here the encoder step size is 25 nm.

A rotation head between camera and microscope is used to align the direction of camera shift and stage motion. The zoom lens can be used to adjust the magnification but

has the disadvantage that the sampling density has to be measured each time.

A Photometrics 200 series camera (Aikens *et al* 1990) is connected to the microscope. This is a slow-scan cooled CCD camera. A Peltier element cools the CCD below  $-35^{\circ}\text{C}$  to suppress dark current. The readout rate is 500 kHz which is slow compared to the 15 MHz of a video camera. An A/D unit converts the collected charge in 12 bits data. The noise level of this camera is photon limited. This means that all other noise sources of the camera are negligible in comparison to the Poisson-

Table 1. Specifications of the CCD elements used with the TDI camera.

	Thompson	Kodak
Type	TH 7882	KAF1400
Element size ( $S \times P$ )	$384 \times 576$	$1317 \times 1035$
Pixel size	$23 \times 23 \mu\text{m}$	$6.8 \times 6.8 \mu\text{m}$
Average (gain <sup>-1</sup> )	$90.9 \text{ e}^-/\text{ADU}$	$7.9 \text{ e}^-/\text{ADU}$
Maximum SNR	56 dB	45 dB
Operating temperature	-35°C	-42°C

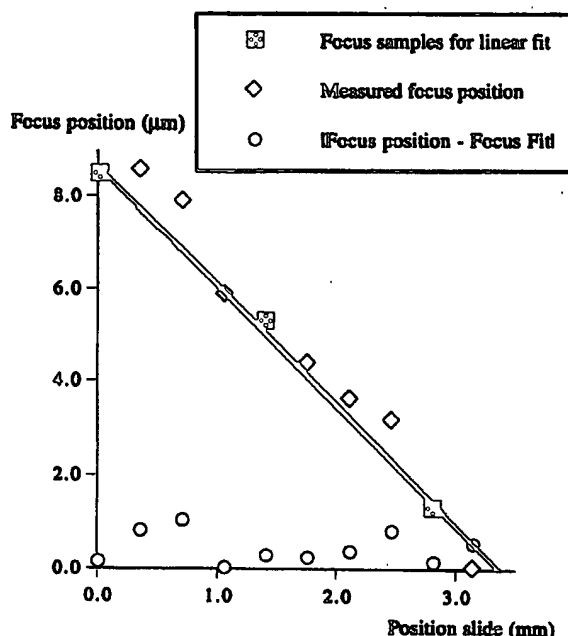


Figure 3. The measured focus position and the result of a linear fit with three focusing samples of a strip of 3.2 mm. The bulbs are the absolute difference between the measured focus position and the linear fit  $z = 8.64 - 2.57x$ . Crossed squares: focus samples for linear fit; diamonds: measured focus position; circles:  $|\text{focus position} - \text{focus fit}|$ .

distributed photon noise. Photometrics provides different CCD elements for the series 200 camera. We have used two cameras with different elements, the Thompson TH 7882 chip and the Kodak KAF1400 chip. Each chip has its own characteristics. The Kodak chip is very large (1.3 Mpixels) and has small pixels. The Thompson chip is comparable to the format of a CCD video camera. The specifications are listed in table 1. The camera control provides the commands for Time Delayed Integration. The external trigger of the camera synchronizes the parallel shift with the stage motion. The camera control can contain between 4 to 32 MByte memory. The data are temporarily stored in the camera control memory, to await further processing. Camera, stage and focus control are connected to a Sun 4/260 computer with an external VME bus.

#### 4.2. TDI scanning in practice

TDI scanning is particularly interesting when large areas have to be scanned. The scanning area is divided into strips. The TDI system images each strip in one scan. Due to the parallel shift of the CCD array there is only one scan direction. After each scan, the stage moves back to the beginning of the next strip.

In the 'dead-time' associated with the mechanical 'fly-back', the stage stops at a small number of places to focus (Boddeke *et al* 1994). These samples are used to stay in focus during the subsequent scan. A linear function is fit to the focusing samples. Figure 3 shows the result of a fit using three focusing samples. The specimen contained DAPI counter stained interphase cell nuclei with a centromeric 8 probe labeled with FITC (provided by the Department of Cytometry and Cytochemistry, Sylvius Laboratory, Leiden University). The length of the strip is 3.2 mm. The linear fit  $z = 8.64 - 2.57x$  defines the focus position during the next scan. The estimated focus position is compared with the measured focus position. The maximum error is 1.1 mm whereas the average absolute error is 0.4 mm. The depth-of-focus of the objective (Nikon 20  $\times$  /0.75) is 0.36 mm (Longhurst 1967). The average error is slightly larger than the depth-of-focus. Experiments have shown that it does not effect the result of spot counting in interphase nuclei (Netten *et al* 1994), but other applications may require a smaller error and have to use more focusing samples.

One scan involves five steps: (1) The stage accelerates to the required speed. (2) The camera opens the shutter and starts shifting the parallel register. (3) The continuous data stream is stored in camera memory. The data can be processed during the scan. The first field of data has to be removed as the pixels of the first field do not shift through the whole CCD element. (4) Disable the camera trigger to stop the parallel shift at the end of the strip. One image is now acquired. (5) The stage moves back to the starting point of the next strip and collects focusing data. These five steps are repeated until the total area is scanned.

For example, to scan an area of  $5 \times 10$  mm with the Kodak chip the system has to acquire a number  $N_s$  of scans each of 10 mm length using the following system setup:

integration time	$T_i = 3 \text{ s}$
objective	Nikon 10 $\times$ /0.5
overall magnification	$M = 25$
pixel size	$D = 6.8 \mu\text{m}$
serial dimension	$S = 1317$
parallel dimension	$P = 1035$ .

The scanning parameters, using equations (1), (2) and (5), are then given by:

spatial sampling frequency	$f_0 = 3.68 \mu\text{m}^{-1}$
parallel shift frequency	$f_p = 345 \text{ Hz}$
stage velocity	$v_0 = 93.8 \mu\text{m s}^{-1}$
scanning speed	$v_{\text{TDI}} = 33.5 \times 10^{-3} \text{ mm}^2 \text{ s}^{-1}$
number of scans	$N_s = (5 \text{ mm}) \times f_0 / S = 14$ .

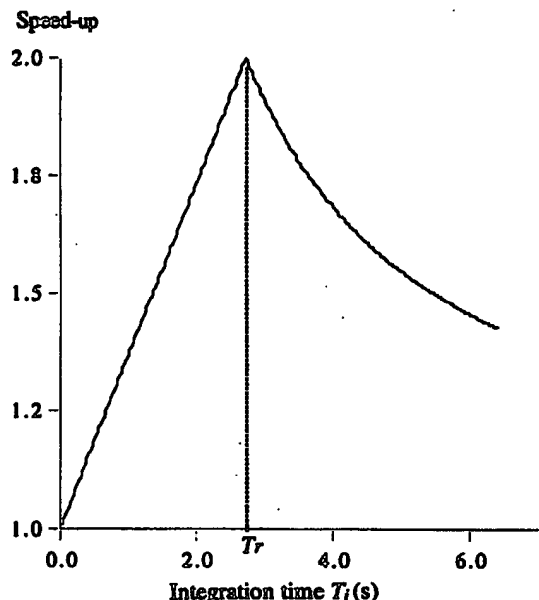


Figure 4. The speed increment of TDI scanning compared to static imaging for the KAF1400 chip. The maximum speedup of 2 is achieved when the integration time is equal to the readout time  $T_r$ .

Each scan takes 110 s, not including the focus time. The acceleration time is 0.1 s per strip, the readout time of the first field is 3 s and moving the stage back takes about 0.5 s per strip. The total scan time is 1540 s in which 680 Mpixels of data are acquired at an effective rate of 442 kHz. Of the 1540 s only  $14 \times (3 + 0.5) = 19$  s or 3.5 % of the total time is spent on initialization and fly-back.

## 5. Performance

To evaluate the performance of TDI scanning, we compare TDI scanning with normal static scanning. The same system is used for both scanning modes, the Photometrics KAF1400 camera. To compare the static to the dynamic approach we examine the improvement in speed and the image quality. The imaging quality is measured in terms of the signal-to-noise ratio (SNR) and spatial frequency response.

### 5.1. Speed increment

One reason to use TDI scanning instead of a start-stop scanning is the speed increment. The speed-up depends on the integration time and the readout time of the camera. The readout time is defined as the time to shift one full field out of the CCD into memory at full rate. Considering (4), speed-up ( $i$ ) is given by:

$$i = \frac{T_i + T_r}{\max(T_i, T_r)} = \begin{cases} 1 + \frac{T_r}{T_i} & T_i > T_r \\ 1 + \frac{T_i}{T_r} & T_r > T_i \end{cases} \quad (6)$$

The numerator defines the time to grab one image with a static system, assuming that the stage moves to the next field during the readout time. The denominator gives the time to collect the data of one field using TDI. The initialization and fly-back times are ignored. Due to the maximum readout rate of the camera, the scanning time per field is limited by the readout time. Figure 4 shows the speedup using the KAF1400 chip. When the integration time is equal to the readout time, TDI scanning gives a maximum speedup of a factor 2. Equation (6) shows that the readout time determines the speed increment for a given integration time. The readout time is equal to the number of pixels divided by the fixed readout rate of 500 MHz for the Photometrics 200 series. The consequence of (6) is that one should select a CCD element (number of rows and columns) that has a readout time that is comparable to the required integration time. TDI scanning then gives the maximum speed increment.

### 5.2. Spatial frequency response

We compared the spatial frequency response of TDI scanning to the response of a static imaging system. The spatial frequency response (SFR) can be estimated by imaging a step edge from which we can derive the overall frequency response of the combined optical system and imaging system (Mullikin *et al* 1994). We used the same camera for static imaging and TDI scanning. Static imaging yields a slightly better spatial frequency response than TDI scanning. The reduction of spatial frequencies has several causes. The continuous motion of the stage versus the discrete shift of the camera causes one-pixel blur in the scan direction of the resulting image. This would be the ideal case when there is a perfect synchronization between stage and camera. A difference in speed will cause additional blurring of the image. Due to the stage motion, vibration of the specimen will smooth the image. Finally if the motion of the stage is not exactly aligned with the CCD shift direction, the image will be blurred perpendicular to the scan direction. To limit the smoothing to half a pixel, the angle between the parallel shift and stage motion must be smaller than  $0.5/P$  rad, where  $P$  is the parallel dimension of the CCD.

Experiments have shown that the degradation of the frequency response perpendicular to the scan direction is not significant. The alignment of the system is very easy to accomplish thanks to the rotation head between the microscope and the camera. Figure 5 shows the overall frequency response in the scan direction of TDI scanning and static imaging. TDI scanning causes a small reduction in spatial frequency response. At a frequency of 1 cycle/mm there is 10 % reduction in resolution; this is hardly visible. The degradation is comparable with 2 pixels blur. If we multiply the spatial frequency response of static imaging with the Fourier transform of a two-pixel wide uniform filter the result is comparable to the spatial frequency response of TDI scanning.

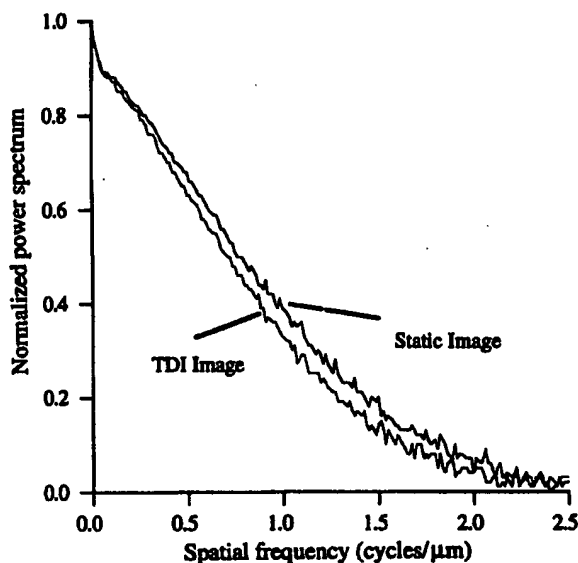


Figure 5. Spatial frequency response in the scan direction for static imaging and TDI scanning. A step edge is imaged using the KAF1400 chip and a Nikon 20 × /0.75 objective. The cut-off frequency of the optical system is 2.7 cycles/mm.

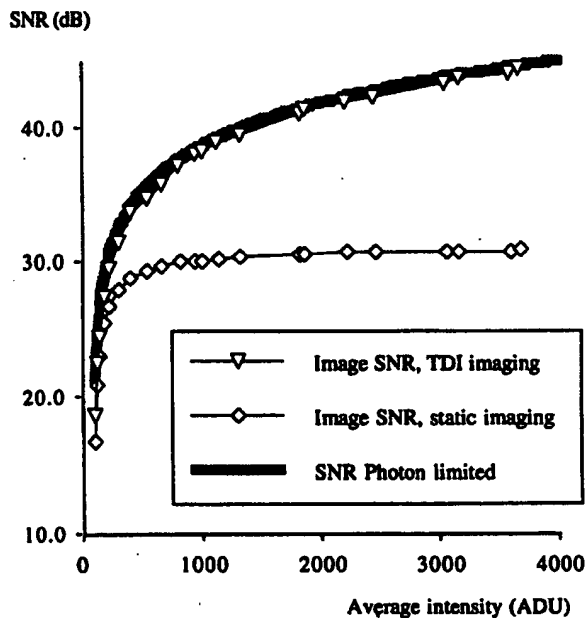


Figure 6. The image SNR of TDI and static imaging for the whole dynamic range of light intensities.

### 5.3. Signal-to-noise ratio

Considering the SNR we distinguish two aspects. First the variation between two or more independent images (pixel

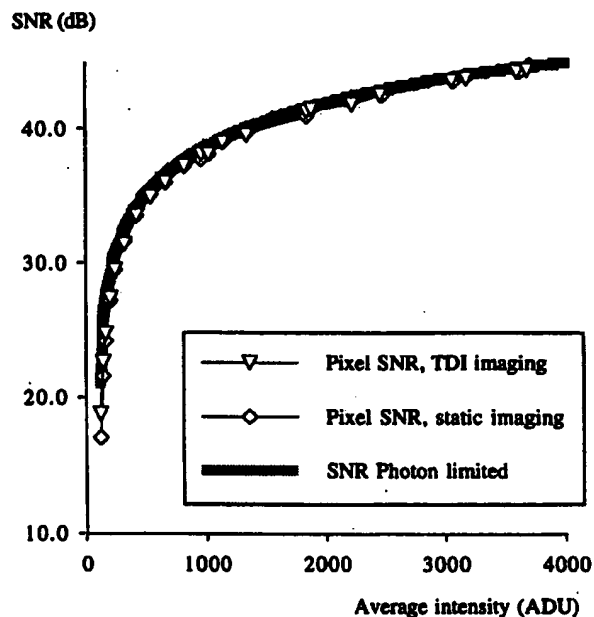


Figure 7. The pixel SNR of TDI and static imaging for the whole dynamic range of light intensities.

SNR) (Mullikin *et al* 1994) and secondly the variation between pixels within a single image (image SNR). The variation between two images with the same illumination is caused by three different sources: readout noise, dark current noise and photon shot noise. This method yields the SNR of an individual pixel illuminated by a stationary light source (pixel SNR). The image SNR is caused by the above listed noise sources in addition to the pixel variation. The pixel variation is caused by a different response of the individual CCD wells to the same amount of light. The SNR is defined as

$$\text{SNR} = 20 \log \left( \frac{\mu}{\sigma} \right) \quad (\text{dB}) \quad (7)$$

where  $\mu$  is the average intensity and  $\sigma$  is the deviation. The variation between two images (average pixel variance) is defined as

$$\sigma_p^2 = \frac{1}{2} \text{var}(I_1 - I_2) \quad (8)$$

where  $I_1$  and  $I_2$  are independent uniformly illuminated images with the same average intensity  $\mu$ . The standard deviation between pixels (image variance) is defined as

$$\sigma_i^2 = \text{var}(I) \quad (9)$$

where  $I$  is a uniformly-illuminated image.

Two uniformly illuminated images were acquired for both TDI and static imaging for a range of intensities. The variations defined in (8) and (9) and the corresponding signal-to-noise ratios were calculated. Figure 6 and figure 7 show the results using the KAF1400 chip. The thick gray line is the ideal SNR of a photon limited camera (a camera





Figure 8. A TDI image of DAPI counter stained cell nuclei. The image size is  $360 \times 3600$  pixels, that is corresponding to an area of  $0.154 \times 1.54 \text{ mm}^2$  on the slide. We have used the TH7882 chip and the Nikon  $60 \times /1.4$  objective.

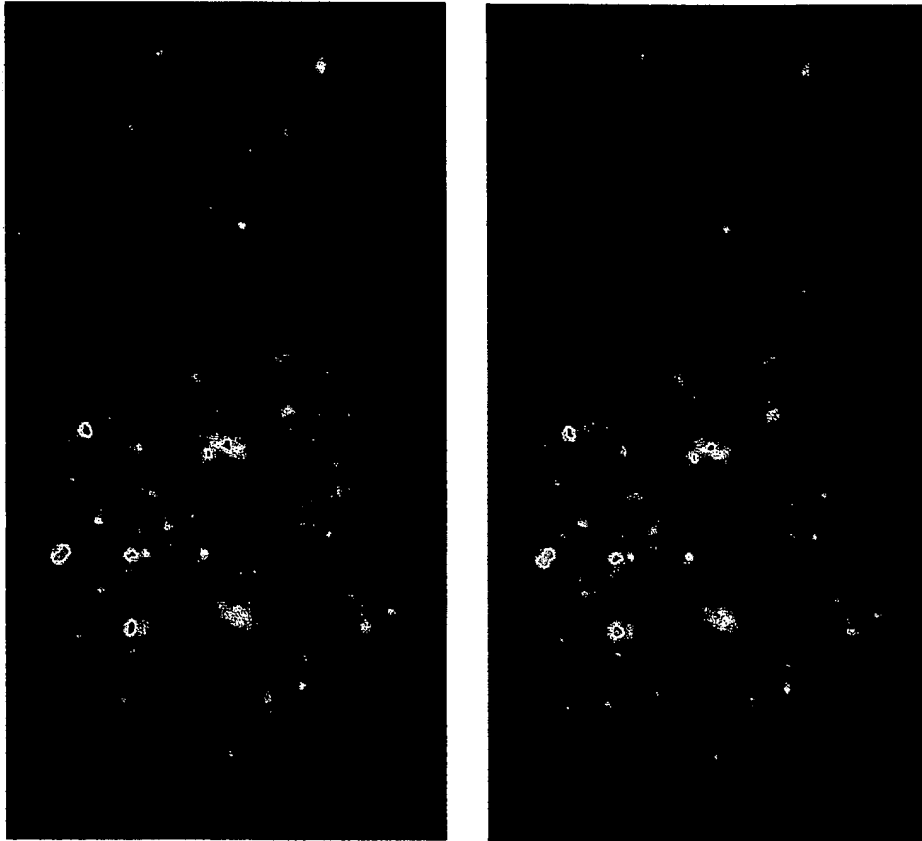


Figure 9. An example of a TDI image ( $229 \times 425$ ) (a) and a static image ( $229 \times 425$ ) (b) of the same microscope field. The images are captured with a Nikon  $60 \times /1.4$  objective and a integration time of 1.2 s.

in which all other noise sources are negligible compared to the photon shot noise induced by the quantum nature of light) and therefore the upper bound for the measured SNR.

In figure 7 we see that the pixel SNR of static and TDI scanning are comparable to the ideal SNR of a the photon limited camera. Other noise sources than photon shot noise are not significant. If there is no variation between the pixels (electron wells) we would expect the same result in figure 6 for the image SNR. However, this is not the case. The image SNR is much lower for a static system. Using TDI scanning one pixel in the output image is an average

over a whole column of electron wells. Therefore the variation is much less and is mainly determined by photon shot noise. It is possible to correct the pixel variation for static imaging using flat field correction. Flat field correction requires a dark field image (shutter closed) and a blank field image (illuminated image without objects) and must be computed using floating point operations. Therefore it is a time consuming operation. If the correction is properly done the image SNR of static imaging will be comparable to TDI imaging.

## 6. Conclusions

We have developed a time-delayed-integration (TDI) CCD scanner suitable for fluorescence microscopy. TDI scanning results in a high data throughput without compromising the image quality. Time delayed integration is achieved by a Photometrics slow scan CCD camera. This camera is available with several different CCD chips. We have evaluated the scanner with two different chips, KAF 1400 and TH 7882. Figure 8 shows an example of scanning one strip of a slide using the TH 7882 chip.

The scanning speed of TDI scanning is at most twice that of static scanning. The required integration time and the readout time of the CCD element determine the speed-up of TDI scanning.

The spatial frequency response (SFR) of TDI scanning is compared with the SFR of a static imaging system. Due to the discrete pixel shift versus continuous motion and synchronization errors there is a small degradation of the spatial frequency response. The resulting blur in the image is comparable with a smoothing filter of  $(2 \times 1)$  pixels and is hardly visible.

TDI scanning provides a complete suppression of pixel variability. The image SNR of TDI scanning is more than 10 dB better than the image SNR of static imaging. Figure 9 shows the results of static and TDI imaging of the same microscope field. Visually there is hardly any difference.

Besides the improved SNR, TDI scanning has the advantage that there is shading in only one direction (perpendicular to the scan direction). Another advantage is that the number of image edges is less than with static imaging. The data throughput is therefore higher because fewer objects touch the image border and no overlap in the scan direction is necessary.

## Acknowledgments

We are grateful to our colleagues from the Department of Cytometry and Cytochemistry, (Sylvius Laboratory, Leiden University, The Netherlands) for providing us with fresh FISH preparations. This work was partially supported by The Netherlands Organization of Biomedical Research (NWO-MW), grant 900-538-016, NATO grant RG.85/0324 and Imagenetics (Naperville, Illinois, USA).

## References

- Aikens R S, Agard D A and Sedat J W 1990 Solid-state imagers for microscopy *Fluorescence Microscopy of Living cells in Culture Part A* ed L Taylor and Y Wang (New York: Academic) pp 291-313
- Barbe D F 1976 *Time Delay and Integration Image Sensors* (Leiden: Nordhoff)
- Boddeke F R, van Vliet L J, Netten H and Young I T 1994 Autofocusing in microscopy based on image formation and sampling *Bioimaging* 2 193-203

- Carter N P 1994 Cytogenetic analysis by chromosome painting *Cytometry* 13 2-10
- Chamberlain S G and Washburn W D 1990 High speed, low noise, fine resolution TDI CCD imagers *SPIE Charge-Coupled Devices and Solid State Optical Sensors* 1242 252-262
- Longhurst R S 1967 *Geometrical and Physical Optics* (London: Longmans)
- Mullikin J C, van Vliet L J, Netten H, Boddeke F R, van der Peltz G *et al* 1994 Methods for CCD camera characterization *Proc. SPIE Image Acquisition and Scientific Imaging Systems, San Jose* 2173 73-84
- Netten H, Young I T, Prins M, van Vliet L J, Tanke H J *et al* 1994 Automation of fluorescent dot counting in cell nuclei *Proc. 12th Int. Conf. on Pattern Recognition Jerusalem, Israel* in press
- Schlig E S 1986 A TDI charge-coupled imaging device for page scanning *IEEE J. of Solid-State Circuits* SC-21 182-6
- Stark M, Farrow S, McKie M and Rutovitz D 1989 Automatic high resolution digitisation of metaphase cells for aberration scoring and karyotyping *Automation of Cytogenetics* ed C Lundsteen and J Piper (Berlin: Springer) pp 31-43
- Tucker J H, Husain O A N, Watts K, Farrow S, Bayley R *et al* 1987 Automated densitometry of cell populations in a continuous motion imaging cell scanner *Appl. Opt.* 26 3315-24
- Warwick K and Rees D 1988 *Industrial Digital Control Systems* (London: Peter Peregrinus)